Technical Sciences
Academy of Romania
www.jesi.astr.ro

Journal of Engineering Sciences and Innovation
Volume 4, Issue 1 / 2019, pp. 17 - 30

A. Mechanical Engineering

Received ***17 December 2018*** *Accepted* ***27 March 2019***
Received in revised from ***28 February 2019***

Polyurethane foam behavior in mixed mode bending

CONSTANTINESCU DAN MIHAI[1,*], **APOSTOL DRAGOŞ ALEXANDRU**[1], **STUPARU FLORIN ADRIAN**[1]

[1]*University POLITEHNICA of Bucharest, Splaiul Independenţei nr. 313, 060042 Bucharest, Romania*

Abstract. Mixed mode four-point bending testing is performed on polyurethane foams. This paper presents only the results on the stress intensity factors (SIFs) obtained experimentally for a density of 325 kg/m^3, although tests were done for three foam densities. An asymmetric four-point bending setup was used for determining the critical SIFs in Mode I and Mode II, and discussions on the influence of the initial crack length on the SIF values are done. As initial crack length is increased the theoretical predictions give a better comparison to experimentally obtained results. Mode II testing is also performed on a polyurethane foam as a particular case of mixed-mode four-point testing. Crack initiation and propagation in Mode II depends on the geometrical parameters of the testing configuration. Numerical XFEM simulations are done in order to clarify the situations in which the crack doesn't propagate, and failure is produced in the region of supports. A combined experimental-XFEM analysis is recommended to fully understand the particularities of the behavior of cellular materials.

Keywords: mixed-mode, polyurethane foam, asymmetric four-point bending, mode II, XFEM, crack propagation.

1. Introduction

Aeronautical, automotive or naval structural integrity is of great importance and any presence of imperfections can reduce significantly the load bearing capacity. Polyurethane (PUR) foam materials are widely used as cores in sandwich composites, for packing and cushioning. They are made of interconnected networks of solid struts and cell walls incorporating voids with entrapped gas. The main characteristics of foams are lightweight, high porosity, high crushability, and good

* Correspondence address: dan.constantinescu@upb.ro

energy absorption capacity, [1,2]. Foam materials, used extensively in such applications, crush in compression, while in tension fail usually by propagation of a single crack, [3]. However, without a better understanding of progressive failure, the fracture criteria and predictive capabilities will be limited. Interface cracking is generally a mixed mode cracking, as both normal and shear stresses develop just ahead of the crack tip, [4, 5]. Experiments have shown that fracture energy can depend on mode mixity [6-8].

Consequently, the fracture toughness of such foams became an important characteristic, because cracks weaken the foam structures capacity of carrying load. Many experimental efforts have been made in recent years to determine the fracture toughness of different types of foams: plastic [9-12], carbon [13] and metallic [14, 15]. McIntyre and Anderson [16], using single edge notch bend specimens made of rigid closed-cell polyurethane foams, measured the K_{Ic} for different densities. They found that the fracture toughness is independent of crack length and proposed a linear correlation between fracture toughness and density, for foam densities smaller than 200 kg/m^3. At higher densities the correlation became non-linear. The same behavior was observed by Danielsson [17] on PVC Divinycell foams and Viana and Carlsson on Diab H foams, [10]. Brittle fracture without yielding produced in Mode I was observed in these experiments. Kabir et al. [12] used the procedure described by ASTM D5045 [18] for determining the fracture toughness of polyvinyl chloride (PVC) and polyurethane (PUR) foams. They investigated the effects of density, specimen size, loading rate and of cell orientation. Density has a significant effect on fracture toughness, which increases more than 7 times when the foam density increases 3.5 times. They also presented the results of the established fracture toughness for H130 foams measured with crack orientation in two directions: rise and flow. The fracture toughness is higher with 27% when the crack is orientated parallel to the rise direction.

The influence of the initial crack length on the values of the stress intensity factors (SIFs) in mixed mode by using a four-point bending configuration is studied in this paper. Obtained values are compared with those given by using well-established criteria and comments on particularities of the obtained results are done. Present paper assesses the toughness of a polyurethane foam and analyzes the crack initiation and propagation by combining experimental and numerical analyses.

2. Comments on XFEM formulation

The eXtended Finite Element Method (XFEM) is an extension of the FEM, and its fundamental features were described by Belytschko and Black [19], based on the idea of partition of unity presented in [20], which consists on local enrichment functions for the nodal displacements to model crack growth and separation between crack faces. With this technique, discontinuities such as cracks are simulated as enriched features, by allowing discontinuities to grow through the enrichment of the degrees of freedom of the nearby nodes with special displacement functions. As the crack tip changes its position and path due to

loading conditions, the XFEM algorithm creates the necessary enrichment functions for the nodal points of the finite elements around the crack path/tip. Compared to cohesive zone modelling (CZM), XFEM excels in simulating crack onset and growth along an arbitrary path without the requirement of the mesh to match the geometry of the discontinuities neither remeshing near the crack, [21]. In [22], Moës et al. used XFEM to create a technique for simulating crack propagation in two dimensions without remeshing the domain. Later Moës and Belytschko [23] integrated CZM into the XFEM framework to overcome the CZM shortcoming because the XFEM is particularly effective in dealing with moving arbitrary discontinuities. Developments were done by Sukumar et al. in [24], where the two-dimensional enrichment functions for planar cracks were used, and afterwards the idea was extended to three dimensions by Areias and Belytschko, [25].

The implementation of the eXtended Finite Element Method in commercial FEA software is still limited, and the most famous one including such capabilities is Abaqus™ (Abaqus Unified FEA). However, due to its relatively recent introduction, XFEM technique in Abaqus™ has been proved to provide trustable results only in few simple benchmark problems involving linear elastic material models.

2. Mixed mode formulation in four-point bending

The experiments in mixed mode are done on established setups, one of the most common being the four-point bend specimen. This can create the pure mode I or II and the mixed modes I and II. The four-point bend specimen is loaded in two forms: symmetric and asymmetric. The symmetric bend specimen creates the pure mode I and the mixed mode, but the asymmetric specimen creates mode II in addition to the mixed modes I and II. In [26] a fundamental reference solution is given for an infinitely long cracked specimen loaded by a constant shear force and the corresponding bending moment. Small corrections need to be applied for a finite four-point loading geometry. Initial tests were already reported, [27], showing the difficulties to perform such tests. In the present paper results on the mode I and mode II stress intensity factors are presented for different geometry configurations of the experimental setup.

Asymmetric four-point bending represents a good method to determine de Mode II stress intensity factor for an isotropic material. The method itself has been investigated by many researchers, but He and Hutchinson [26] have thoroughly studied it and even proposed corrections that consider the ratio between the length of the initial crack and the height of the sample. These corrections are suitable for ratios less than 0.5, but by increasing it the values of the corrections no longer influence the main results.

The formulas that are used to determine the values of the stress intensity factors for each mode are, [26]:

$$K_I^R = \frac{6cQ}{W^2}\sqrt{\pi a}F_I\left(\frac{a}{W}\right), \tag{1}$$

$$K_{II}^R = \frac{Q}{W^{\frac{1}{2}}}\frac{\left(\frac{a}{W}\right)^{\frac{3}{2}}}{\left(1-\frac{a}{W}\right)^{\frac{1}{2}}}F_{II}\left(\frac{a}{W}\right) \tag{2}$$

The experimental setup is presented in Fig 1 and consists of two four point bending fixtures positioned in an asymmetric configuration.

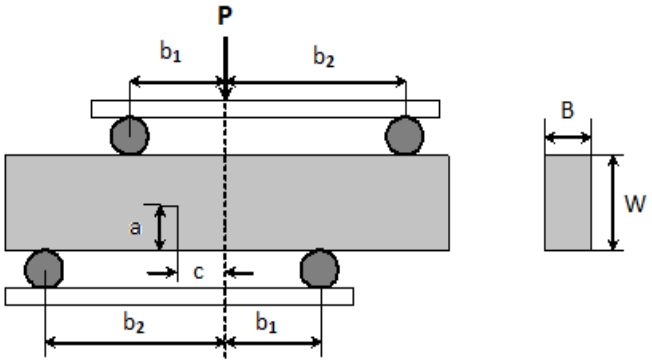

Fig. 1. Experimental setup for four-point bending.

In relations (1) and (2) the force P gives the shear force Q which acts between the inner loading points is given by $Q = P\,(b_2 - b_1)/(b_2 + b_1)$ and $M = cQ$ is the moment. All tested specimens had B = 12.5 mm, W = 25 mm, and $b_1 + b_2$ = 100 mm. In this paper, crack length a to height W ratios are 0.5 and 0.68.

The reference solution of Eqs. 1 and 2 is accurate (finite element results show this in [27]) if the distance of the nearest loading point is greater than 1.4W. That is $(b_1 - c) > 1.4W$. For our b_1 value (initially considered as 40 mm) results c < 5 mm, as to fulfill this condition. For loading points nearer to the crack, He and Hutchinson established that a correction of the above relations is needed, as these are valid only for a reference specimen.

It is relatively clear that if parameter c is chosen to be zero, mode I will no longer influence the test, thus the setup will lead to a shear load, resulting a mode II crack propagation. The ration between crack length a and the height of the sample W is considered when each stress intensity factor is being calculated upon using the following relations:

$$F_I\left(\frac{a}{W}\right) = 1.122 - 1.121\left(\frac{a}{W}\right) + 3.740\left(\frac{a}{W}\right)^2 + 3.873\left(\frac{a}{W}\right)^3 - 19.05\left(\frac{a}{W}\right)^4 + 22.55\left(\frac{a}{W}\right)^5 \tag{3}$$

$$F_{II}\left(\frac{a}{W}\right) = 7.264 - 9.37\left(\frac{a}{W}\right) + 2.74\left(\frac{a}{W}\right)^2 + 1.87\left(\frac{a}{W}\right)^3 - 1.04\left(\frac{a}{W}\right)^4. \quad (4)$$

3. Experimental testing

All specimens were produced by cutting them from a panel of polyurethane foam with density 325 kg/m^3. The polyurethane foam is named Necuron 301, produced by Necumer. The crack has been produced artificially by using a razor blade and cutting the foam to the desired initial crack length *a*.

The tests have been performed on a Zwick-Roell Z010 testing machine, capable of measuring a force up to 10 kN. The distance between the supports has been four times the height of the sample, that is 100 mm. The purpose of these tests was to determine the variation of the stress intensity factors with respect to parameter *c*. Speed of testing was always considered as being 1 mm/min, [16].

The specimens were tested using different values for the parameter *c*, by considering its values in the range specified for each tested setup. As an example, for Setup 2 we tested for values of *c* equal to 1, 2.5, 4.5 and 7. For each selected value of parameter *c* we considered a minimum of five tests in order to validate the results, [28]. The setups used are presented in Table 1.

Table 1. Setups used for ratio a/W = 0.5 and W = 25 mm.

Dimension	Setup 1	Setup 2	Setup 3
b_1 [mm]	40	42.5	45
b_2 [mm]	60	57.5	55
B [mm]	12.5	12.5	12.5
c [mm]	< 5	< 7.5	< 10

By using these setups, we were able to determine the stress intensity factors presented in Fig. 2. The results show that there is a little difference between the values obtained for *c* being 1 and 2.5, and we can even say that for c = 2.5 the Mode II values increase a little bit suggesting that it could be a problem in propagating the crack correctly.

Another important draw back represented the fact that the cracks don't propagate at all in some cases, especially for Setup 3, where the difference between b_2 and b_1 is approaching the value of 10. For this case the samples started to break in the supports' region due to the crushing of the foam in that area.

The stress intensity factors obtained experimentally are normalized to the mode I fracture toughness and compared to the theoretical predictions obtained with consecrated criteria: maximum circumferential tensile stress (MTS), minimum strain energy density (SED), maximum energy release rate (G_{max}), equivalent stress intensity factor (ESIF). Thus, for each criterion, a curve represents the failure locus for Mode I and Mode II cohabitation.

The results obtained from experimental data of valid tests (for some tests the crack didn't propagate) are represented in Fig. 3; the experimentally obtained ratios K_{II}/K_{Ic} are to be represented as a function of K_I/K_{Ic}, and then are compared to the theoretical ones.

As one can notice the values are well below the proposed criteria for establishing the critical locus of failure, and this comparison suggests that the crack didn't propagate correctly. Therefore, we decided to increase the ratio to $a/W = 0.68$.

Another issue is related to the fact that some specimens broke near the supports, which cannot lead to a valid test. We decided to increase the difference between b_2 and b_1 and started to perform tests for b_1= 37.5 mm instead of b_1= 45 mm, as an example. The setup configurations are presented in Table 2.

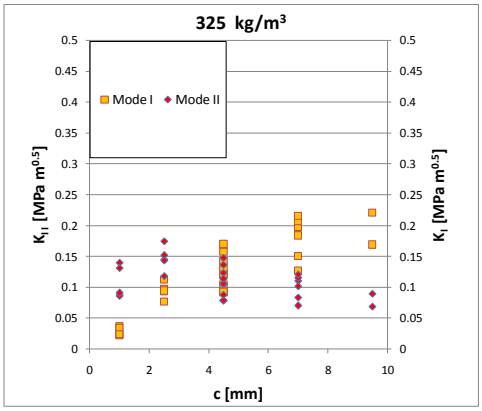

Fig. 2. Stress intensity factors for Mode I and Mode II function of c, for $a/W = 0.5$ and $W = 25$ mm.

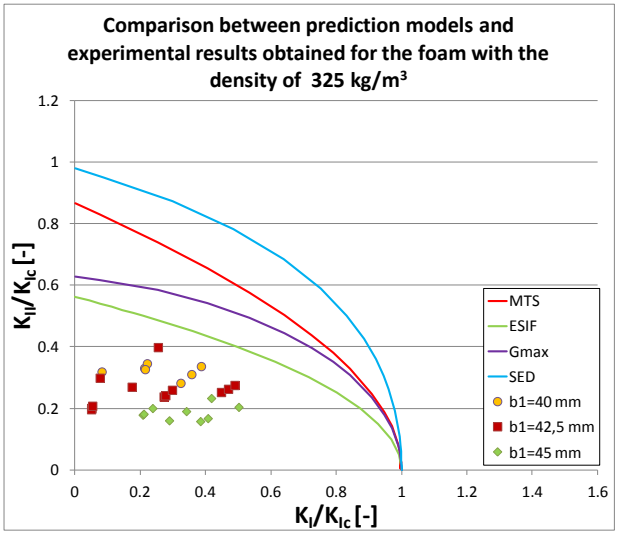

Fig. 3. Variation of normalized SIFs compared to the theoretical predictions for $a/W = 0.5$ and $W = 25$ mm.

Table 2. Setups used for ratio a/W = 0.68 and W = 25 mm.

Dimension	Setup 1	Setup 2	Setup 3
b_1 [mm]	37.5	40	42.5
b_2 [mm]	62.5	60	57.5
B [mm]	12.5	12.5	12.5
c [mm]	<2.5	< 5	< 7.5

Using these configurations, we were able to perform valid tests by determining the critical stress intensity factor (toughness) in Mode II for c = 0, and afterwards by increasing each time with 2 mm the value of the parameter c. The variation of the SIFs was obtained for all the testing setups. By taking this decision the results improved significantly, as to be seen in Fig. 4.

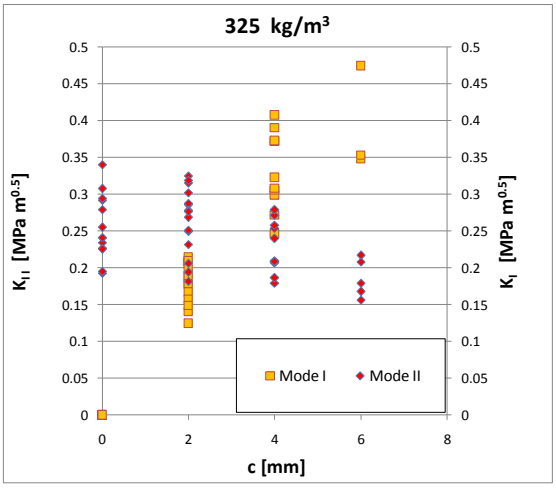

Fig. 4. Stress intensity factors for Mode I and Mode II function of c, for a/W = 0.68 and W = 25 mm.

Even if the results are quite scattered, a pattern of variation is to be noticed clearly, mainly that Mode I SIFs increase with parameter c while Mode II SIFs decrease with this parameter. This is a normal behavior as Mode I values are proportional to the parameter c.

To validate these tests, by plotting the experimentally obtained values together with those given by the theoretical criteria, one can observe in Fig. 5 that the results improved considerably and can be predicted using some of the already mentioned criteria.

The results obtained for using the highest values of c for b_1 = 40 mm and b_1 = 42.5 mm fall outside the prediction criteria which suggest the fact that the crack propagated in an unstable manner.

By increasing W to a value of 30 mm, we studied again the phenomena observed previously, trying to understand what happens for extreme values of parameter c. In Table 3 the experimental setups are presented.

Table 3. Setups used for ratio a/W = 0.68 and W = 30 mm.

Dimensions	Setup 1	Setup2	Setup3	Setup 4	Setup 5
b_1 [mm]	42.5	45	47.5	50	52.5
b_2[mm]	77.5	75	72.5	70	67.5
B [mm]	12.5	12.5	12.5	12.5	12.5
c [mm]	< 0.5	< 3	< 5.5	< 8	<10.5

Again, we should remember that condition $(b_1 - c) > 1.4W$ must be fulfilled. For the b_1 values (given in Table 3) limitations for c values do result.

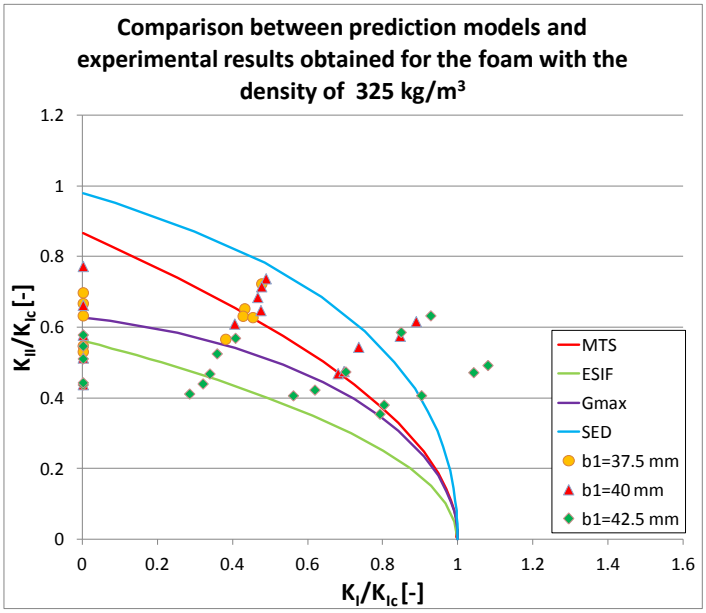

Fig. 5. Variation of normalized SIFs compared to the theoretical predictions for a/W = 0.68 and W = 25 mm.

The stress intensity factors obtained experimentally are normalized to the mode I fracture toughness and compared to the theoretical predictions as mentioned before. Thus, for each criterion, results a curve which represents the failure for Mode I and Mode II cohabitation. By using the configurations described in Table 3 the obtained results were plotted in Fig. 6.

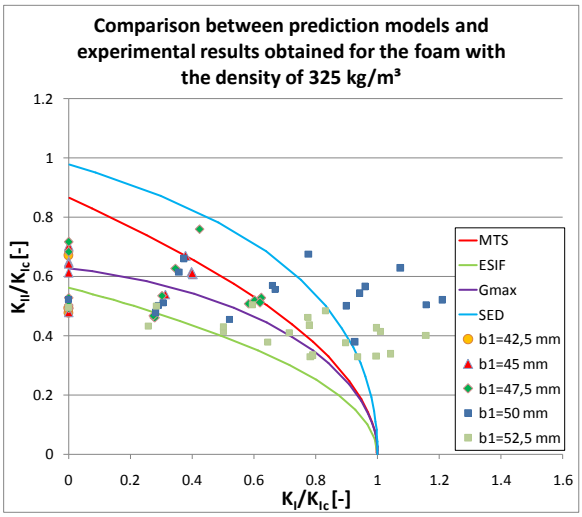

Fig. 6. Test results plotted against prediction models for a/W = 0.68 and W = 30 mm.

The obtained results revealed that there is a dependency between the crack propagation and the b_1 distance. This means that by increasing the distance b_1 the results are starting to become more scattered and for c close to the maximum limits the obtained results are not following any criteria. Starting from this conclusion we describe a critical distance as being $\delta = b_2 - b_1$ for which the crack will not propagate, or it will propagate under certain special conditions.

For tests performed using δ = 20 mm and c = 0 we observed that the crack did propagate for one test, but the values were not predictable by any criteria, while for δ = 15 mm we were unable to propagate correctly the crack for three values, as c = 0, 2 and 4 mm.

Even if the experimental results results can be explained for extreme values of the parameter c, where mode mixity is fully dependent as parameter c multiplies Mode I SIF value, they don't explain why the crack doesn't propagate for certain conditions.

In order to investigate and clarify this issue we performed XFEM simulations for the tested setups.

4. XFEM analysis of crack propagation

Constructing a good 2D XFEM model requires knowing how the analyzed material performs under different loading conditions. Compression, tensile and fracture toughness data obtained from experiments are used in order to construct the model that will help investigate the behavior of the studied foam under mixed-mode testing.

The model functions upon a simple requirement, that is initiating a crack when a certain maximum principal strain value is achieved. By calculating all the time this

value the crack is initiated and then propagated on a direction. The maximum principal strain is found to be usually equal to the strain at which the foam breaks in tension.

The cellular material has been analyzed using the hyperfoam model from Abaqus™ by inserting tabular compression testing data, that will be used to describe the crushing behavior of the material in the supports and loading areas.

The damage evolution is defined by the released energy *G* (crack driving force), and represents the area enclosed by the stress and strain curve for the element.

Because we are dealing with a mixed mode situation the *G* energy represents the equivalent energy which is consumed in order completely propagate the crack. The formula which gives the condition of propagation is written as

$$\left(\frac{G_I}{G_{Ic}}\right)^n + \left(\frac{G_{II}}{G_{IIc}}\right)^n = 1\,. \tag{5}$$

In this power law relation, we considered that *n* is equal to 1 for this application, while G_{Ic} and G_{IIc} are the critical values for the released energy determined in Mode I and Mode II.

Tensile and fracture toughness tests results have been used in order to calculate the values needed for relation (1) and presented in Table 4.

Table 4. Input data for the numerical model.

E [MPa]	ν [-]	K_{Ic} [MPa$\sqrt{m}$]	K_{IIc} [MPa$\sqrt{m}$]	Maximum principal strain [-]
282	0.31	0.34	0.31	0.073

Using the input data, we were able to fully understand the behavior of the material when performing tests for W = 30 mm in the case of Setups 4 and 5 (Table 3), [29]. The load is applied by considering a displacement control loading and measuring the reaction forces that appear in the support region. In order to propagate the crack, it is compulsory to determine the stress values that appear in the loading vicinity and support areas. This is done by creating a tie node that sums all the forces that are measured in this region.

In Fig. 7 one can observe that the equivalent stress values are well above the crushing and shear values of the material, reaching approximately 18 MPa.

Crack propagates with a sudden change of direction, thus suggesting a brittle behavior of the material. The model can analyze the crack propagation during mixed mode testing, being able to describe the crack path for any *c* value. The model revealed that in order to propagate a crack in the sample a very high force value is needed when testing in Setups 4 and 5 configurations, as it is to be seen in Fig. 8.

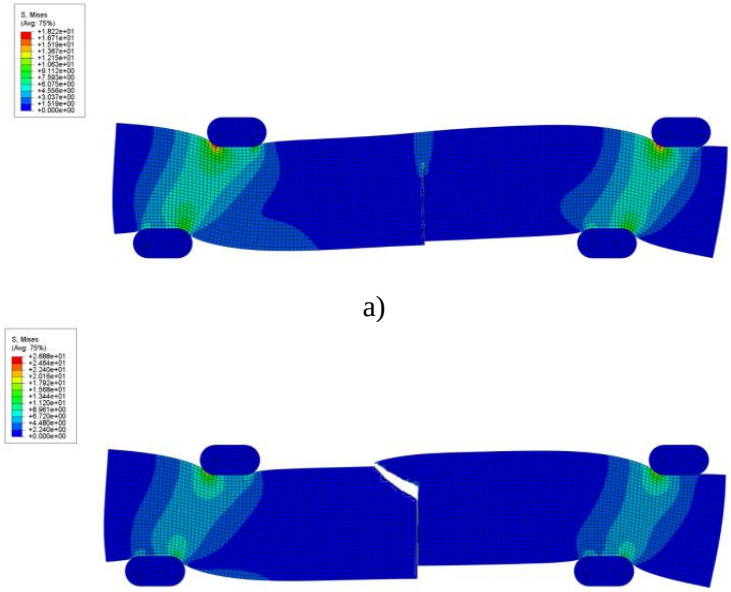

a)

b)

Fig. 7. Von Mises stress values at: a) initiation; b) full propagation of the crack.

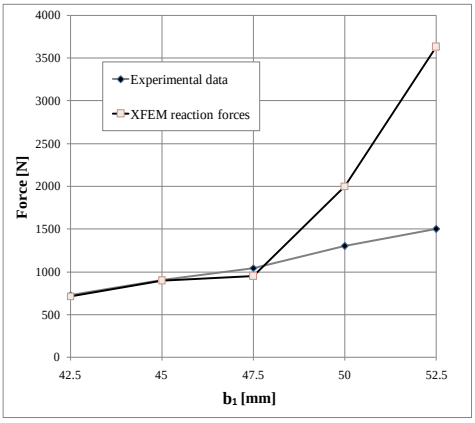

Fig. 8. Comparison between experimental and XFEM data.

In Fig. 8 the experimental data has been obtained by calculating and plotting the mean values of the forces obtained in the experiments. This is a usual practice, but the standard deviation values should be considered especially when testing an anisotropic material because for a particular setup one can obtain a broad range of force values which can be justified by the anisotropy or by the fact that the crack was blunt or different defects were present inside the material.

One of the most important characteristics of the numerical model is that it can describe what happens in some cases when crack propagates in the support or

loading region. The model approximated correctly what happens for values b_1 = 42.5, 45 and 47.5 mm, as with the decrease of δ the model requires a larger value of the force in order to propagate the crack. We observed that this value cannot be reached since in the same time the crack propagates in the loading area and it becomes dominant.

In order to perform all these analyzes one must understand how XFEM propagates a crack based on the critical *G* energy. The parameter called StatusXFEM can take values from 0 to 1 and represents the amount of the *G* energy that has been used to propagate the crack through an element. This parameter is used to understand what happens in the loading region, as to be noticed in Fig. 9.

In Fig. 9 a) the von Mises stress values are quite high in the support region, leading to the development of new cracks. This is supported by the fact that in Fig. 9 b) one can observe that almost the entire region is subjected to high stresses, the StatusXFEM variable is almost 0.5 (green color elements), crack being initiated, but as soon as value 1 (red color elements) is reached the crack is propagated. This means that the energy has been consumed to propagate a crack in the loading and support region and this is found to happen also in the experimental setups for δ equal to 15 and 20 mm.

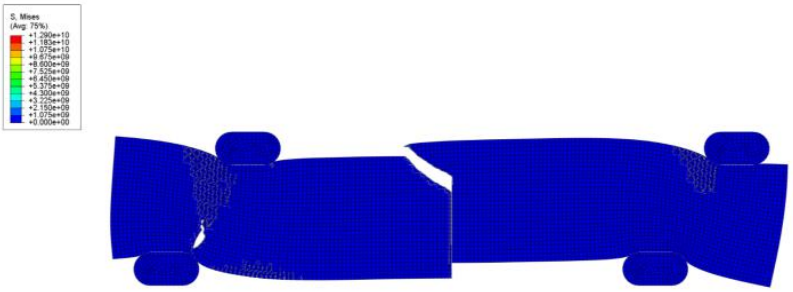

a)

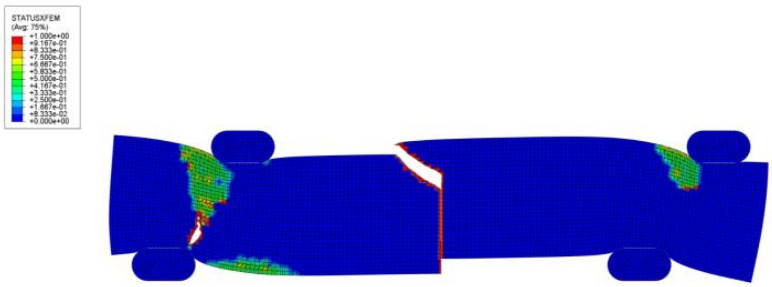

b)

Fig. 9. Crack propagated in the support and loading region:
a) von Mises stress values; b) XFEM element status.

6. Conclusions

Mixed-mode testing of a polyurethane foam is done by using a four-point bending configuration. The crack propagation is monitored and corresponding SIF values in Mode I and Mode II are calculated. The experimental results of normalized SIFs are compared to the those obtained by theoretical predictions, using well-established criteria. It was found that the geometrical configuration of the specimen and of the testing device makes difficult the crack propagation for the initial ratio a/W = 0.5, damage and failure in the loading area becoming dominant. By increasing the crack length and corresponding ratio a/W = 0.68, it is to be underlined that, although a scatter of data exists, the experimental critical SIFs can be established.

Some theoretical criteria can predict quite correctly the normalized values of SIFs, but usually Richard's criterion (ESIF) is the one that predicts better the behavior of cellular materials, as a polyurethane foam.

Mixed mode testing of polyurethane foams is in some situations followed by undesired failure in the region of supports without any propagation of the main crack. In Mode II testing it is sometimes difficult to propagate the crack due to the geometrical constrains of the testing configuration. Some of the experimental results obtained for SIFs are not comparable to the theoretical predictions.

XFEM simulations are done to study the crack initiation and propagation and explain the failure produced in the supports' region and not in the vicinity of the main crack. This numerical approach proves to be a powerful method of analysis if the model is correctly calibrated. Therefore, a combined experimental-XFEM analysis can lead to proper results for assessing the failure of polyurethane foams in various loading conditions.

References

[1] Gibson L.J., Ashby, M.F., Cellular Solids, Structure and Properties, 2nd edition, Cambridge University Press, Cambridge, 1997.
[2] Mills N.J., Polymer Foams Handbook: Engineering and Biomechanics Applications and Design Guide, Elsevier, Oxford, 2007.
[3] Marsavina L., Constantinescu D.M., Failure and damage in cellular materials, in Failure and Damage Analysis of Advanced Materials, CISM International Centre for Mechanical Sciences, Eds. Holm Altenbach, Tomasz Sadowski, Volume 560, p. 119-190, Springer, Vienna, 2015.
[4] Williams M.L., The stress around a fault or crack in dissimilar media, Bull. Seismo. Soc. Am., **49**, 1959, p. 199-204.
[5] Rice J.R., Elastic fracture mechanics concepts for interfacial cracks, Trans. J. Appl. Mech., **55**, 1988, p. 98-103.
[6] Cao H.C, Evans A.G., An experimental study of the fracture resistance of bimaterial interfaces, Mech. Mater., **7**, 1989, p. 295-304.
[7] Wang J.S., Suo Z., Experimental determination of interfacial toughness curves using Brazil-nut-sandwiches, Acta Metall., **38**, 1990, p. 1279-1290.
[8] Liechti K.M., Chai Y.S., Asymmetric shielding in interfacial fracture under in-plane shear, Trans. ASME J. Appl. Mech., **59**, 1992, p. 295-304.

[9] Fowlkes C.W., Fracture toughness of a rigid polyurethane foam, Int. J. Fract., 10, 1974, p. 99-108.
[10] Viana G.M., Carlsson L.A., Mechanical properties and fracture characterization of cross-linked PVC foams, J. Sandw. Struct. Mater., **4**, 2002, p. 99-113.
[11] Burman M., Fatigue crack initiation and propagation in sandwich structures, Report No. 98-29, Stockholm, 1998.
[12] Kabir M.E., Saha M.C., Jeelani S., Tensile and fracture behavior of polymer foams, Mat. Sci. Eng. A, **429**, 2006, p. 225-235.
[13] Choi S., Sankar B.V., Fracture toughness of carbon foam, J. Compos. Mater., 37, 2003, p. 2101-2116.
[14] Fleck N.A., Olurin O.B., Chen C., Ashby M.F., The effect of hole size upon the strength of metallic and polymeric foams, J. Mech. Physics Solids, **49**, 2001, p. 2015-2030.
[15] Olurin O.B., Fleck N.A., Ashby M.F., Deformation and fracture of aluminium foams, Mat. Sci. Eng. A, **291**, 2000, p. 136-146.
[16] McIntyre A., Anderton, G.E., Fracture properties of a rigid PUR foam over a range of densities, Polymer, **20**, 1979, p. 247-253.
[17] Danielsson M., Toughened rigid foam core material for use in sandwich construction, Cell. Polym., **15**, 1996, p. 417-435.
[18] ASTM D5045-99: Standard Test Methods for Plane-Strain Fracture Toughness and Strain Energy Release Rate of Plastic Materials, ASTM International, West Conshohocken, PA, USA.
[19] Belytschko T., Black T., Elastic crack growth in finite elements with minimal remeshing, Int. J. Fract., **45**, 1999, p. 601-620.
[20] Melenk J.M., Babuska I., Seminar fur Angewandte Mathematik, Eidgenos sische Technische Hochschule, Research Report No. 96-01, January, Zurich, Switzerland, 1996.
[21] Campilho R.D.S.G., Banea M.D., Chaves F.J.P., da Silva L.F.M., eXtended Finite Element Method for fracture characterization of adhesive joints in pure mode I, Comput. Mater. Sci., **50**, 2011, p. 1543-1549.
[22] Moës N., Dolbow J., Belytschko T., A finite element method for crack growth without remeshing, Int. J. Numer. Meth. Engng., **46**, 1999, p. 131-150.
[23] Moës N., Belytschko T., Extended finite element method for cohesive crack growth, Engng. Fract. Mech., **69**, 2002, p. 813-833.
[24] Sukumar N., Moës N., Moran B., Belytschko T., Extended finite element method for three- dimensional crack modelling, Int. J. Numer. Meth. Engng., **48**, 2000, p. 1549-1570.
[25] Areias P., Belytschko T., Analysis of three-dimensional crack initiation and propagation using the extended finite element method, Int. J. Numer. Meth. Engng., **63**, 2005, p.760-788.
[26] He M.Y., Hutchinson J.W., Asymmetric four-point crack specimen, J. Appl. Mech., **67**, 2000, p. 207-209.
[27] Shahani A.R., Tabatabei S.A., Computation of mixed mode stress intensity factors in a four-point bend specimen, Appl. Mater. Modell., **32**, 2008, p. 1281-1288.
[28] Apostol D.A., Constantinescu D.M., Marşavina L., Linul E., Mixed-mode testing for an asymmetric four-point bending configuration of polyurethane foams, Appl. Mech. Mater., **760**, 2015, p. 239-244.
[29] Apostol D.A., Stuparu F.A., Constantinescu D.M., Marşavina L., Linul E., Experimental and XFEM analysis of mode II propagating crack in a polyurethane foam, Materiale Plastice, **53**, 2016, p. 685-688.